



**HAL**  
open science

## Experimental investigation of wall-pressure fluctuations on a full-scale business jet

Edouard Salze, Simon Prigent, Emmanuel Jondeau, Christophe Bailly

### ► To cite this version:

Edouard Salze, Simon Prigent, Emmanuel Jondeau, Christophe Bailly. Experimental investigation of wall-pressure fluctuations on a full-scale business jet. e-Forum Acusticum 2020, Dec 2020, Lyon, France. pp.727-730, 10.48465/fa.2020.0255 . hal-03229449

**HAL Id: hal-03229449**

**<https://hal.science/hal-03229449>**

Submitted on 21 May 2021

**HAL** is a multi-disciplinary open access archive for the deposit and dissemination of scientific research documents, whether they are published or not. The documents may come from teaching and research institutions in France or abroad, or from public or private research centers.

L'archive ouverte pluridisciplinaire **HAL**, est destinée au dépôt et à la diffusion de documents scientifiques de niveau recherche, publiés ou non, émanant des établissements d'enseignement et de recherche français ou étrangers, des laboratoires publics ou privés.

# EXPERIMENTAL INVESTIGATION OF WALL-PRESSURE FLUCTUATIONS ON A FULL-SCALE BUSINESS JET

Édouard Salze   Simon Prigent   Emmanuel Jondeau   Christophe Bailly

École Centrale de Lyon, 36 avenue Guy de Collonge, 69131 Écully, France

edouard.salze@ec-lyon.fr

## ABSTRACT

In cruise conditions, the velocity fluctuations throughout the turbulent boundary layer induce wall-pressure fluctuations on the fuselage, which contribute to a large part of cockpit and cabin noise. Flight tests are regularly performed by airplane manufacturers but the complexity and the cost of such tests usually make it difficult to extract detailed informations under well-controlled conditions. In the framework of Cleansky 2 H2020 CANOBLE Project, an experiment was conducted to analyze cockpit and cabin noise on a full-scale fuselage of a Dassault Aviation business jet, in an industrial-size wind tunnel. Boundary layer profiles have been characterised by means of hot-wires. An array of hot films was also used for the analysis of wall shear stress. The local pressure gradients in the regions of interest were extracted using a network of 70 static pressure probes, all over the fuselage. Arrays of 128 digital MEMS microphones, stuck onto the fuselage, served for the measurement of the wall-pressure excitation. All these results should contribute in the derivation and validation of wall-pressure models.

## 1. INTRODUCTION

Wall-pressure fluctuations beneath turbulent boundary layers are involved in many topics : flow-induced vibration, structural damages, air and ground transportation, submarine detection, etc. This topic has therefore attracted the attention of researchers in the last decades [1–4]. For an aircraft in cruise conditions, the wall-pressure fluctuations induced on the fuselage by the turbulent boundary layer is an important contributor to cockpit and cabin noise. In the near future, with the development of quieter propulsion, such as ultra-high bypass ratio engines, or distributed propulsion, the relative contribution of the turbulent boundary layer is expected to grow more. In the framework of Cleansky 2 H2020 program, a project called CANOBLE (CAbin NOise from Boundary Layer Excitation) was launched with Dassault Aviation, Vibratéc, the wind-tunnel S2A, and École Centrale de Lyon, to progress towards a better understanding of the wall-pressure excitation, the vibro-acoustic transmission through the fuselage, and the acoustic radiation inside the cabin. With that objective, a realistic full-scale model of the cockpit and cabin of a business jet was designed, built, and instrumented to perform experiments in a large scale wind tun-

nel. The present paper focuses on the external measurements of wall-pressure excitation on the full-scale mock-up.

## 2. EXPERIMENTAL SET-UP

The configuration of the present study is the fore part of a Dassault Aviation Falcon 2000 business jet. This set-up is around 10 m long in total. The first 6 m have been built in true scale and in true geometry, compared to a real aircraft. The remaining 4 m serve as a tail to streamline the rear part of the mock-up (see Fig. 1).

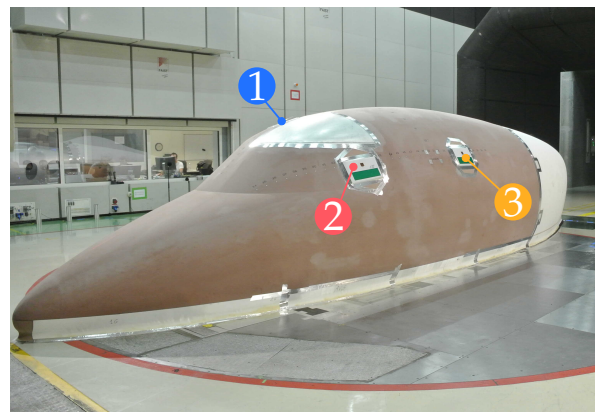


**Figure 1.** Experimental apparatus in the S2A large-scale wind-tunnel, with the position of instrumented modules 1, 2 and 3.

The fuselage of the aircraft was instrumented in three different locations :

- the roof, identified as **module 1**
- the windscreen, identified as **module 2**
- the side panel, identified as **module 3**

As is sketched in Fig. 2, each of the 3 instrumented modules has been equipped with static pressure probes to measure the pressure gradient, a thermocouple to measure the temperature, 4 hot films to extract the wall-shear stress, an access to perform velocity profiles using a hot wire, a flush-mounted 1/8 inch GRAS type 40DP condenser microphone, to serve as a reference microphone, and 40 digital MEMS microphones mounted on a flexible PCB. The microphones arrays are built using pairs of digital Invensense INMP621 microphones with a PDM output.

Each array comprises 40 microphones with a non-uniform distribution, whose signals are synchronously recorded during 2 min at the sample rate of 50 kHz. More details about the microphones arrays can be found in a recent paper by some of the present authors [5]. This instrumentation was fit flush on a 3D printed thin flare which was stuck onto the fuselage.

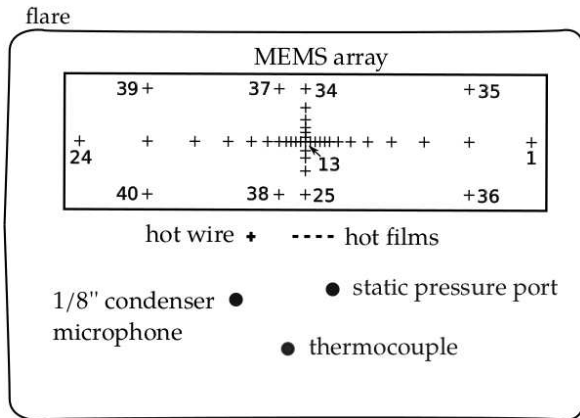


**Figure 2.** Instrumented modules stuck onto the fuselage.

The experiment was conducted in the S2A full-scale aeroacoustic wind-tunnel, near Paris. This facility has an open-jet wind tunnel with a cross-sectionnal area of 24 m<sup>2</sup> and a maximum flow speed around 70 m.s<sup>-1</sup>. In this paper, only results at 30 m.s<sup>-1</sup> are presented, additional results can be found in a recent paper from the present authors [6].

### 3. RESULTS

#### 3.1 Turbulent boundary layer characterisation

Boundary layer profiles have been estimated over 20 measurement points at distances between 0.1 mm and 12 cm away from the fuselage. For each measurement point, 20 seconds of signal are acquired at the sample rate of 102.4 kHz. Mean velocity profiles have been expressed in wall units and plotted in figure 3. The boundary layers of modules 1 and 2 exhibit similar profiles, which is expected for those two regions which are at relatively similar distances from the aircraft nose. The outer region of module 3 is more developed, as module 3 is located further downstream. Characteristic values extracted from those profiles (boundary layer thicknesses, friction velocities, etc.) are indicated in Table 1 together with the pressure gradient parameters extracted from the static pressure measurements.

In the log region of the velocity profiles (see Fig. 3), longer recordings of 2 minutes have been performed at the sample rate of 102.4 kHz so as to extract well-converged velocity spectra. Under the Taylor assumption [7], the one-dimensionnal spectrum of longitudinal velocity fluctuations  $E_{(11)}^1(k_1)$  is estimated from the experimental spectra  $\Phi_{(11)}(f)$  as

$$E_{(11)}^1 = \Phi_{(11)} \frac{U_1}{2\pi} \quad \text{with} \quad k_1 = \frac{2\pi f}{U_1}$$

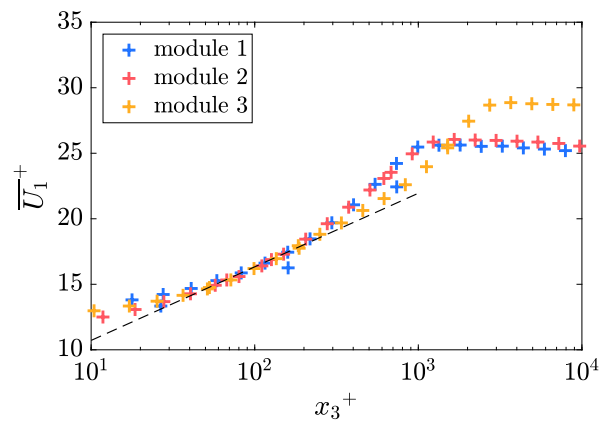


**Figure 3.** Mean velocity profiles expressed in wall units, measured on the fuselage at 30 m.s<sup>-1</sup>.

$U_\infty$ (m/s)	$\delta_1$ (mm)	$\delta$ (mm)	$H$ -	$u_\tau$ (m/s)	$Re^+$ -	$\beta$ $\times 10^2$	$L$ (mm)
33.6	1.84	11.5	1.35	1.30	955	1.2	18.1
32.1	2.18	14.8	1.34	1.24	1170	-6.8	19.2
31.2	5.84	37.0	1.35	1.09	2620	6.4	56.3

**Table 1.** Boundary layer parameters, extracted from the velocity profiles of figure 3 : free-stream velocity  $U_\infty$ , displacement thickness  $\delta_1$ , boundary layer thickness  $\delta$ , shape factor  $H$ , friction velocity  $u_\tau$ , Reynolds number  $Re^+ = u_\tau \delta / \nu$ , pressure gradient Clauser parameter  $\beta$ , and the correlation length of longitudinal velocity fluctuations  $L$ .

The one-dimensional spectra are then compared to the von Karman spectrum model with a good agreement (see Fig.4). This model can be used later in wall-pressure models with a reasonable fidelity.

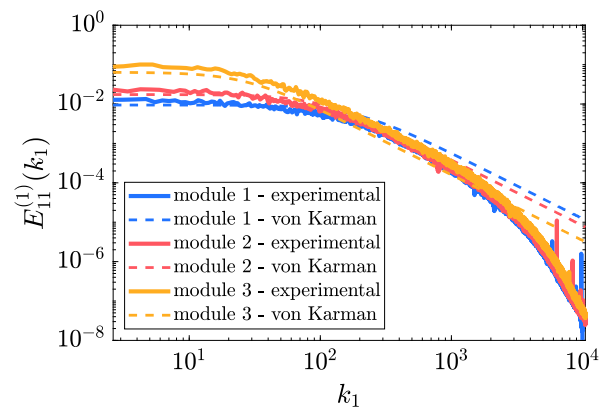


**Figure 4.** One-dimensional experimental velocity fluctuations spectra  $E_{11}^1$ , compared to the one-dimensional von Karman model.

#### 3.2 Wall-pressure fluctuations

Wall-pressure fluctuations are recorded using digital MEMS microphones arrays located on each module. The signals are split into blocs of 250 ms and the spectra and cross-spectra are computed using the periodogram method, with a Hann windowing and a 50% overlap between seg-

ments. The resulting spectra appear in Figure 5. The hump, located around  $\omega\delta_1/U_\infty=8$ , is due to the resonance of the MEMS pressure port [6]. Because the Clauser parameter obtained at module 1 is close to zero (see Table 1), indicating a nearly zero-pressure-gradient boundary layer, the parameters from module 1 have been chosen to feed the Goody model proposed in Figure 5. The good agreement obtained enables the use of a Goody model in a numerical simulation, for instance.

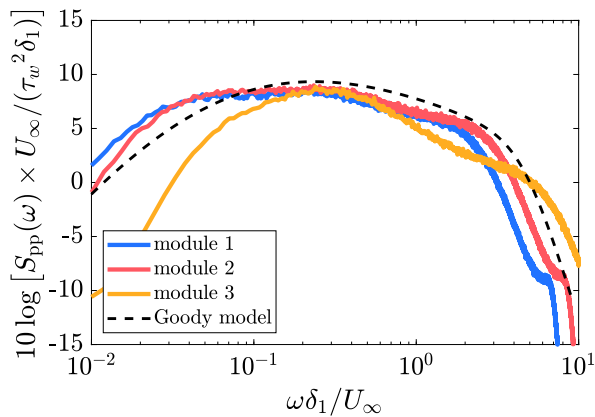


**Figure 5.** Wall-pressure spectra  $S_{pp}$ , normalised by mixed variables, compared to the Goody model.

The coherence between pressure signals is then computed using the cross-spectra, up to 5 kHz. The resulting two-dimensional coherence surface is shown at the frequency of 500 Hz in Figure 6. In this figure, color blue indicates a coherence close to 1, whereas color red indicates a coherence close to zero. As was predicted by Corcos [1], the coherence function is rapidly decreasing with the distance. The decrease rate is faster in the spanwise direction than is the streamwise direction. In order to accurately measure this decrease, the microphone array was equipped with two lines of microphones, spanwise and streamwise.

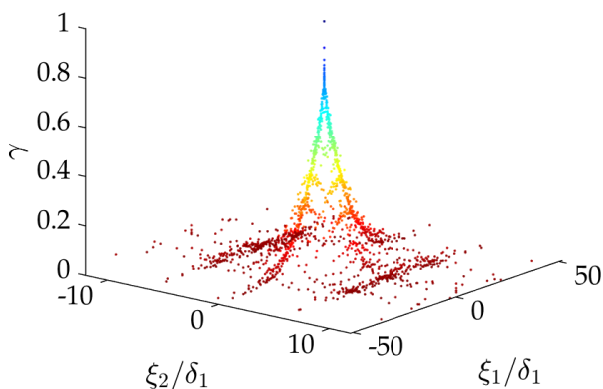


**Figure 6.** Coherence between microphone, obtained using the cross-spectra measured at 500 Hz on module 3.

The two-dimensional wavenumber spectra can then be

obtained through the spatial Fourier transform of the cross-spectra [8, 9]. The resulting two-dimensional spectrum is presented at 500 Hz, for module 3, in figure 7. As was obtained in other studies by some of the present authors, the main contribution to the wall-pressure spectra is the convective ridge associated to the hydrodynamic pressure fluctuations in the turbulent boundary layer. This contribution is found at the convective wavenumber  $k_c = 2\pi f/U_c = 144 \text{ rad.m.}^{-1}$ , which is consistent with the wavenumber spectrum of Figure 7. In this example, the convection velocity  $U_c$  is roughly estimated at 70% of the free-stream velocity  $U_\infty$ . The contribution of the lower wavenumbers does not appear at this frequency in this experiment, but was documented in some other measurements with the same apparatus [5].

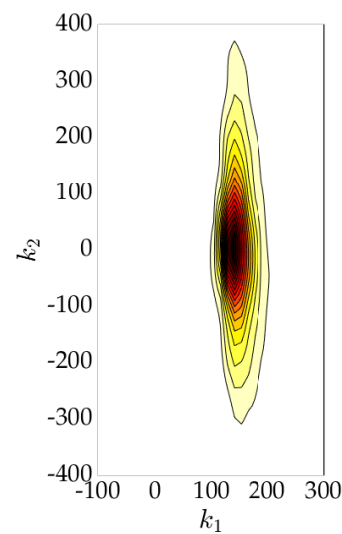


**Figure 7.** Two-dimensional wavenumber spectrum  $\Phi_{pp}(k_1, k_2, \omega)$  obtained at 500 Hz from the module 3.

#### 4. CONCLUSION

In the framework of Cleansky 2 H2020 program, a detailed wall-pressure experiment was performed on a full-scale representative cabin and cockpit of a Dassault Aviation business jet. The dedicated aerodynamic instrumentation (hot wire and hot films, static pressure ports) provided reliable and detailed data on the structure of the boundary layers. The velocity profiles, friction velocities, wall-shear stresses, and correlation lengths of the velocity fluctuations have been obtained. In particular, the velocity spectra can be represented with a good agreement using a von Karman model whose parameters were extracted from the experiment to serve later in numerical computations. MEMS microphones arrays were used to extract wall-pressure spectra, coherence, and wavenumber spectra. Some results have not been presented in this paper, but the wall-pressure measurements enabled the extraction of convection velocities, correlation lengths of the pressure fluctuations. The pressure spectra can be represented by a good agreement

using a Goody model in the region of low pressure gradient, which is convenient for engineering purposes. However, the regions of higher pressure gradients will need a dedicated modelling, which will be the goal of future studies.

## 5. ACKNOWLEDGEMENTS

This project has received funding from the Clean Sky 2 Joint Undertaking under the European Union's Horizon 2020 research and innovation programme under grant agreement N°717084.

This work was performed within the framework of the Labex CeLyA of the Université de Lyon, within the programme "Investissements d'Avenir" (ANR-10-LABX-0060/ANR-16-IDEX-0005) operated by the French National Research Agency (ANR).

The authors would like to thank Floriane Rey from Dassault Aviation, Romain Leneveu and Hugo Siwiak from Vibratex, for coordinating the overall project and overseeing the manufacturing of the mock-up. The authors are also grateful to their colleague Pascal Souchotte for his support throughout the project.

## 6. REFERENCES

- [1] Corcos, G. M., 1964, The structure of the turbulent pressure field in boundary-layer flows, *J. Fluid Mech.*, **18**(3), 353–378.
- [2] Blake, W.K., 1986, Essentials of turbulent wall-pressure fluctuations, in Mechanics of flow-induced sound and vibration, Vol. II Complex flow-structure interactions, *Academic Press Inc.*, Orlando, Florida.
- [3] Bull, M.K., 1996, Wall-pressure fluctuations beneath turbulent boundary layers: some reflections on forty years of research, *J. Sound Vib.*, **190**(3), 299–315.
- [4] Abraham, B. M. & Keith W. L., 1998, Direct measurements of turbulent boundary layer wall pressure wavenumber-frequency spectra, *J. Fluid Eng.*, **120**, 29–39.
- [5] Salze, E., Jondeau, E., Pereira, A., Prigent, S. & Bailly, C., 2019, A new MEMS microphone array for the wavenumber analysis of wall-pressure fluctuations: application to the modal investigation of a ducted low-Mach number stage, 25th AIAA/CEAS Aeroacoustics Conference, <https://arc.aiaa.org/doi/abs/10.2514/6.2019-2574>.
- [6] Prigent, S., Salze, E., Jondeau, E., & Jondeau, E., 2020, Spatial structure and wavenumber filtering of wall pressure fluctuations on a full-scale cockpit model, *Experiments in Fluids*, 61:201, <https://doi.org/10.1007/s00348-020-03017-2>.
- [7] Bailly, C. & Comte-Bellot, G., 2015, *Turbulence*, Springer, ISBN 978-3-319-16159-4, <https://www.springer.com/gp/book/9783319161594>.
- [8] Arguillat, B., Ricot, D., Bailly, C., & Robert, G., 2010, Measured wavenumber: Frequency spectrum associated with acoustic and aerodynamic wall pressure fluctuations, *The Journal of the Acoustical Society of America* 128(4), 1647–1655, doi:10.1121/1.3478780.
- [9] Salze, É., Bailly, C., Marsden, O., Jondeau, E., & Juvé, D., 2014, An experimental characterisation of wall pressure wavevector-frequency spectra in the presence of pressure gradients. In: 20th AIAA/CEAS Aeroacoustics Conference, p. 2909 (2014). doi:10.2514/6.2014-2909